

Crystal growth and magnetic properties of quantum spin liquid candidate $KErTe_2$

Weiwei Liu(刘维维), Dayu Yan(闫大禹), Zheng Zhang(张政), Jianting Ji(籍建葶), Youguo Shi(石友国), Feng Jin(金峰), and Qingming Zhang(张清明)

Citation: Chin. Phys. B, 2021, 30 (**10**): 107504. DOI: 10.1088/1674-1056/ac1574
Journal homepage: http://cpb.iphy.ac.cn; http://iopscience.iop.org/cpb

What follows is a list of articles you may be interested in

Spin orbit torques in Pt-based heterostructures with van der Waals interface

Qian Chen(陈倩), Weiming Lv(吕伟明), Shangkun Li(李尚坤), Wenxing Lv(吕文星), Jialin Cai(蔡佳林), Yonghui Zhu(朱永慧), Jiachen Wang(王佳晨), Rongxin Li(李荣鑫), Baoshun Zhang(张宝顺), and Zhongming Zeng(曾中明)

Chin. Phys. B, 2021, 30 (**9**): 097506. DOI: 10.1088/1674-1056/ac0908

Optimized growth of compensated ferrimagnetic insulator $Gd_3Fe_5O_{12}$ with a perpendicular magnetic anisotropy

Heng-An Zhou(周恒安), Li Cai(蔡立), Teng Xu(许腾), Yonggang Zhao(赵永刚), and Wanjun Jiang(江万军)

Chin. Phys. B, 2021, 30 (**9**): 097503. DOI: 10.1088/1674-1056/ac0db0

Effective model for rare-earth Kitaev materials and its classical Monte Carlo simulation

Mengjie Sun(孙梦杰), Huihang Lin(林慧航), Zheng Zhang(张政), Yanzhen Cai(蔡焱桢), Wei Ren(任玮), Jing Kang(康靖), Jianting Ji(籍建葶), Feng Jin(金峰), Xiaoqun Wang(王孝群), Rong Yu(俞榕), Qingming Zhang(张清明), and Zhengxin Liu(刘正鑫)

Chin. Phys. B, 2021, 30 (**8**): 087503. DOI: 10.1088/1674-1056/ac0a5d

Some experimental schemes to identify quantum spin liquids

Yonghao Gao(高永豪), Gang Chen(陈钢)

Chin. Phys. B, 2020, 29 (**9**): 097501. DOI: 10.1088/1674-1056/ab9df0

The variation of Mn-dopant distribution state with *x* and its effect on the magnetic coupling mechanism in $Zn_{1-x}Mn_xO$ nanocrystals

Cheng Yan, Hao Wei-Chang, Li Wen-Xian, Xu Huai-Zhe, Chen Rui, Dou Shi-Xue

Chin. Phys. B, 2013, 22 (**10**): 107501. DOI: 10.1088/1674-1056/22/10/107501

Crystal growth and magnetic properties of quantum spin liquid candidate $KErTe_2$*

Weiwei Liu(刘维维)[1,†], Dayu Yan(闫大禹)[2,†], Zheng Zhang(张政)[1], Jianting Ji(籍建葶)[2], Youguo Shi(石友国)[2,‡], Feng Jin(金峰)[2,§], and Qingming Zhang(张清明)[2,3]

[1] *Department of Physics and Beijing Key Laboratory of Opto-electronic Functional Materials and Micro-nano Devices, Renmin University of China, Beijing* 100872, *China*

[2] *Beijing National Laboratory for Condensed Matter Physics, Institute of Physics, Chinese Academy of Sciences, Beijing* 100190, *China*

[3] *School of Physical Science and Technology, Lanzhou University, Lanzhou* 730000, *China*

(Received 21 April 2021; revised manuscript received 4 June 2021; accepted manuscript online 18 July 2021)

Recently rare-earth chalcogenides have been revealed as a family of quantum spin liquid (QSL) candidates hosting a large number of members. In this paper we report the crystal growth and magnetic measurements of $KErTe_2$, which is the first member of telluride in the family. Compared to its cousins of oxides, sulfides and selenides, $KErTe_2$ retains the high symmetry of $R\bar{3}m$ and Er^{3+} ions still sit on a perfect triangular lattice. The separation between adjacent magnetic layers is expectedly increased, which further enhances the two dimensionality of the spin system. Specific heat and magnetic susceptibility measurements on $KErTe_2$ single crystals reveal no structural and magnetic transition down to 1.8 K. Most interestingly, the absorption spectrum shows that the charge gap of $KErTe_2$ is roughly 0.93±0.35 eV, which is the smallest among all the reported members in the family. This immediately invokes the interest towards metallization even superconductivity using the compound.

Keywords: quantum spin liquids, exchange and superexchange interactions, magnetic anisotropy

PACS: 75.10.Kt, 75.30.Et, 75.30.Gw **DOI:** 10.1088/1674-1056/ac1574

1. Introduction

Quantum spin liquid is a novel quantum state in which no spontaneous symmetry break occurs even at zero temperature.[1] After the discovery of high temperature superconductivity (HTS), Anderson tried to apply the QSL picture to understand the mechanism of HTS. It was proposed that when doped with holes, the resonating valence bond is a singlet state with coherent mobile carriers and is indistinguishable in terms of symmetry from a singlet BCS superconductor. Based on this idea, many theoretical concepts have been proposed to understand the connection between QSLs and high-temperature superconductivity, for example, the spin–charge separation (holon and spinon),[2] the slave-boson theory,[3] and the mean-field theory.[4–7]

Experimentally, several compounds with spin $S = 1/2$, such as herbertsmithite ($ZnCu_3(OH)_6Cl_2$), $YbMgGaO_4$, and α-$RuCl_3$, have been proven to be QSL candidates.[8–21] However, most of them suffer from one or more problems (such as site disorder, interlayer exchange interactions, or antisymmetric Dzyaloshinsky–Moriya (DM) interactions[22,23]) which make these systems complex to explore. For example, the recently discovered $YbMgGaO_4$ has a perfect triangular lattice structure ($R\bar{3}m$)[11–14,16,24,25] with the adjacent triangle layers having a relative large distance. Thus, the interlayer exchange interactions and the DM interactions can be ignored in this system. However, it still suffers from the issue of Ga/Mg disorder, which was suggested to be responsible for the disordered spin state and/or QSL stability.[11,26–28]

Recently, we discovered the family of rare-earth chalcogenides $ARECh_2$ (A = alkli or monovalent ions, Re = rare earth, Ch = O, S, Se, Te) as QSL candidates, which has attracted much attention since these systems inherit almost all the advantages of $YbMgGaO_4$, but do not suffer from the site disorder issue.[29–34] The compounds have a high symmetry with space group $R\bar{3}m$ and the magnetic rare-earth ions form triangular layers that are well separated.[29] Compared with transition metal ions, the 4f rare-earth ions with odd number of electrons have stronger spin orbital couplings and are protected by time reversal symmetry (Kramers doublets). Thus, they can be treated as an ion with effective spin $S = 1/2$ on the crystalline-electronic field (CEF) ground state. Moreover, the huge difference of radii of the cations makes the site disorder impossible. Thus, the rare-earth chalcogenides family $ARECh_2$ (A = alkli or monovalent ions, Re = rareearth, Ch = O, S, Se, Te) provide a platform to study QSLs.

On the other hand, it is noted that with increasing the ra-

*Project supported by the National Key Research and Development Program of China (Grant Nos. 2017YFA0302904 and 2016YFA0300504), the National Natural Science Foundation of China (Grant Nos. U1932215 and 11774419), the Strategic Priority Research Program of the Chinese Academy of Sciences (Grant No. XDB33010100), and Postdoctoral Science Foundation of China (Grant No. 2020M670500), Q.M.Z. acknowledges the support from Users with Excellence Program of Hefei Science Center and High Magnetic Field Facility, CAS.

†These authors contributed equally.

‡Corresponding author. E-mail: ygshi@aphy.iphy.ac.cn

§Corresponding author. E-mail: jinfeng@iphy.ac.cn

© 2021 Chinese Physical Society and IOP Publishing Ltd

dius of the chalcogen ions, the charge gap Δ decreases, for example, $\Delta_{NaYbO_2} \simeq 4.5$ eV $> \Delta_{NaYbS_2} \simeq 2.7$ eV $> \Delta_{NaYbSe_2} \simeq 1.9$ eV.[29] Then it is interesting to ask what will happen if the chalcogen ions are replaced by bigger ions (such as Te^{2-}). Particularly, is it possible to realize the crossover from QSL to metallization even superconductivity? This basically motivates the present work.

In this paper, we report the successful synthesis of a new rare-earth chalcogenide compound $KErTe_2$. It shares the same structure ($R\bar{3}m$) as $NaYbSe_2$ with the magnetic rare-earth ions forming perfect triangular layers. No structural and magnetic transition are observed down to 1.8 K in susceptibility and specific heat measurements. Moreover, the charge gap of $KErTe_2$ is roughly 0.93±0.35 eV, which is the smallest gap among all QSL candidates. These findings suggest that $KErTe_2$ represents a QSL candidate with much smaller charge gap. Thus, $KErTe_2$ provides a platform on which one can easily tune the charge gap and may have chance to explore the connection between QSLs and high-temperature superconductivity.

2. Experiments and methods

Single crystals of $KErTe_2$ were synthesized by the self-flux method with molar ratio K : Er : Te = 1.5 : 1 : 9. K, Er, and Te elements were put into the carton crucible orderly, then sealed into the quartz tube in vacuum. The quartz tube was annealed at 800 ℃ for 20 h, and then the ampoule was slowly cooled down to 500 ℃ with about 2 ℃/h. Finally, the ampoule was span in a centrifuge. The same processwas also used to successfully grow $KLuTe_2$ single crystals. The obtained $KErTe_2$ single crystal is shown in Fig. 1(a).

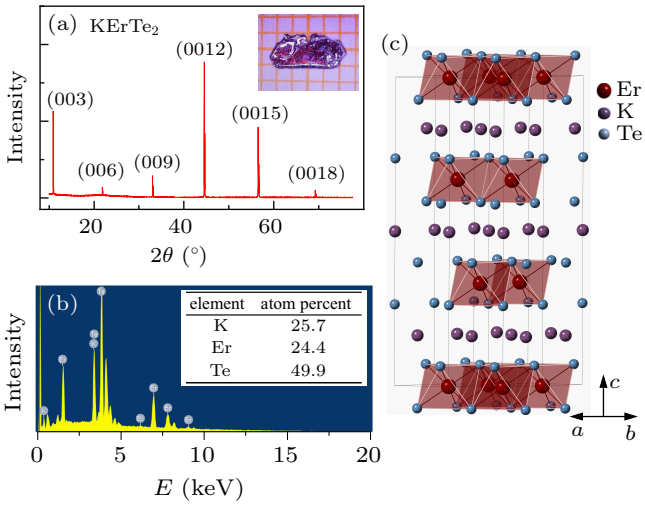


Fig. 1. (a) XRD pattern of $KErTe_2$ single crystal on the (00L) plane. Inset: An image of the synthesized sample. (b) EDX and (c) crystal structure of $KErTe_2$.

After the successful synthesis of single crystals $KErTe_2$, several measurements were used to characterize them, such as x-ray diffractometer (XRD; Bruker-D8), energy-dispersive x-ray spectroscopy (EDX; Oxford X-Max 50), and four-circle single crystal diffractometer (X'Pert3MRD). All these measurements indicate the high quality of the synthesized $KErTe_2$ single crystals and the detailed results will be discussed in the next section.

The magnetic susceptibility and heat capacity measurements were performed using a Quantum Design physical property measurement system (QD PPMS DynaCool) over the temperature range from 1.8 K to 300 K and under magnetic fields of up to 9 T. The absorption spectrum of the sample was collected by a UV-Vis absorption spectrometer (PerkinElmer Lambda 750) to obtain the charge gap of $KErTe_2$.

3. Results and discussion

Figure 1(a) displays the XRD pattern of the synthesized $KErTe_2$ single crystals, and several discrete peaks can be observed. These peaks can be well described by the Bragg equation $2d\sin\theta = n\lambda$ and no other impurity peaks can be observed, indicating the high quality of the synthesized single crystals. In addition, the EDX spectroscopy is used to characterize the atomic ratios of the single crystals (Fig. 1(b)). The determinted average atomic ratios are K : Er : Te = 1.05(3) : 1 : 2.04(5), close to the stoichiometric ratio of $KErTe_2$. All above results indicate the high quality of the synthesized $KErTe_2$ single crystals.

Moreover, we further determined the crystal structure and the lattice parameters of the $KErTe_2$ by x-ray four-circle diffraction. Its space group is $R\bar{3}m$ and the detailed lattice parameters are summarized in Table 1. According to the determined lattice parameters, the schematic structure of $KErTe_2$ is shown in Fig. 1(c), which is isomorphic to $NaYbCh_2$. The magnetic 4f rare-earth Er^{3+} ions form perfect triangular layers that are well separated by nonmagnetic K layers. The distance between the two adjacent triangular layers is 8.131 Å while the nearest neighbor distance between magnetic Er^{3+} ions is 4.4294(9) Å. Due to the larger radius of Te^{2-}, both of these two distances are larger than those of $KErSe_2$.

Table 1. Structural parameters of $KErTe_2$ given by x-ray four-circle diffraction (space group $R\bar{3}m$, No. 166; a = 4.4294(9) Å, and c = 24.392(7) Å).

Atom	x	y	z
K	0	0	0
Er	2/3	1/3	0.83333
Te	1/3	2/3	0.90288

To characterize the behavior of the local moment of Er^{3+}, we first measured the magnetic susceptibility of single crystals $KErTe_2$ (Fig. 2(a)). Down to 1.8 K, no magnetic order/transition can be observed for magnetic fields H applied both in the ab plane ($H//ab$) and along the c-axis ($H//c$). We also examined the magnetic susceptibilities in field cooling (FC) and zero-field cooling (ZFC) measurements. No splitting was detected between the FC and ZFC results down to 1.8 K,

indicating the absence of spin glassy transitions (Fig. 2(a)). These magnetic properties imply that $KErTe_2$ is a perfect platform to study novel magnetic properties in the frustrated system.

To quantify the spin interaction between the Er^{3+} ions, we fit the magnetic susceptibility data with the Curie–Weiss law ($\chi = C/(T - \Theta_{CW})$) to obtain the Curie–Weiss temperature. For the high-temperature range (100–200 K, Fig. 2(b)), the Curie–Weiss fitting yields Curie–Weiss temperature $\Theta_{CW}^{ab} = -0.3$ K and $\Theta_{CW}^{c} = -6.0$ K with $H//ab$ and $H//c$, respectively. However, since the Er^{3+} ions do not stay in the ground state at high temperature, the above Curie temperatures cannot exactly reflect the energy scale of the spin interaction. Then, we try to fit the magnetic susceptibility data at low temperature range (1.8–4 K, Fig. 2(c)) and the obtained Curie–Weiss temperatures are $\Theta_{CW}^{ab} = -0.4$ K and $\Theta_{CW}^{c} = -7.6$ K with $H//ab$ and $H//c$, respectively. More detailed fitting parameters are summarized in Table 2. The negative Curie–Weiss temperatures indicate predominantly antiferromagnetic spin interactions in this system, which is consistent with the absence of hysteresis loop in the M–H curves (Fig. 2(d)). In addition, we can see from the M–H curve that the saturation phenomenon is observed at about 5 T, and the linear behavior occurs above 5 T, which is due to van Vleck paramagnetism.

Figures 2(e) and 2(f) present the temperature-dependent magnetic susceptibility under different magnetic fields with the field $H//ab$ (Fig. 2(e)) and $H//c$ (Fig. 2(f)), respectively. For both directions of the field, the susceptibility $\chi(T)$ shows similar behaviors, decreasing with increasing field. This behavior indicates that huge frustrations in $KErTe_2$ exist at zero field and with increasing field, the frustrations are strongly suppressed. Anyway, the above magnetic measurements suggest that the magnetic Er^{3+} ions are antiferromagnetically coupled with each other and even down to 1.8 K, these local moments are disorderly distributed. Thus, $KErTe_2$ represents a QSL candidate.

Table 2. Parameters extracted from Curie–Weiss fitting for $KErTe_2$.

		C (emu·K·mol^{-1}·Oe^{-1})	Θ_{CW} (K)	μ_{eff} (μ_B)
HT-fitting	$H//ab$	10.811	−0.3	9.3
	$H//c$	10.351	−6.0	9.1
LT-fitting	$H//ab$	9.245	−0.4	8.6
	$H//c$	11.045	−7.6	9.4

To better characterize the ground state of $KErTe_2$, we performed temperature-dependent specific heat measurements on $KErTe_2$ single crystals. As shown in Fig. 3(a), below 10 K, the heat capacity of $KErTe_2$ exhibits a significant different behavior from that of a perfect nonmagnetic reference compound $KLuTe_2$, whose lattice is nearly the same as that of $KErTe_2$. Moreover, it can be found that the heat capacity of $KLuTe_2$ can be well described by the Debye phonon heat capacity model, indicating that it is totally contributed by the lattice. Thus, other contributions to the heat capacity of $KErTe_2$ can be precisely extracted by directly subtracting the lattice contributions, i.e., the heat capacity of $KLuTe_2$ from that of $KErTe_2$. As shown in Fig. 3(b), two broad peaks located at ~ 2 K and ~ 10 K can be well resolved. The origin of these two peaks due to the impurities can be excluded since no impurity signal has been found from the structural and magnetic susceptibility measurements.

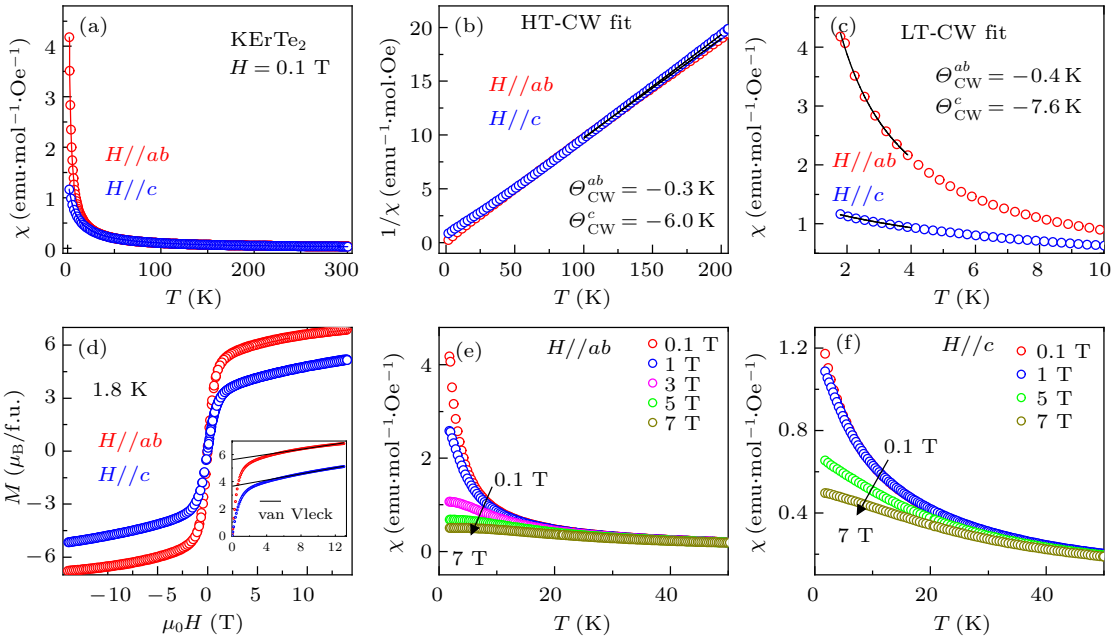


Fig. 2. (a) Temperature-dependence of the magnetic susceptibility $\chi(T)$ measured under zero-field cooling (ZFC, opend circles) and field cooling (FC, solid curves) with the field $\mu_0 H = 0.1$ T applied in the *ab* plane and along the *c* axis. Paramagnetic behavior is observed at low temperature with no obvious differences between ZFC and FC data. (b) Curie–Weiss fitting of the high temperature magnetization data (HT: 100–200 K). The fitting results in Curie temperatures of $\Theta_{CW}^{ab} = -0.3$ K and $\Theta_{CW}^{c} = -6.0$ K. (c) Curie–Weiss fitting of the low temperature magnetization data (LT: 1.8–4 K). The fitting results in Curie temperatures of $\Theta_{CW}^{ab} = -0.4$ K and $\Theta_{CW}^{c} = -7.6$ K. (d) The magnetic hysteresis loop curves of $KErTe_2$ at 1.8 K. The field-dependence of the $\chi(T)$ curves with the field applied (e) in *ab*-plane and (f) along *c* axis is also shown.

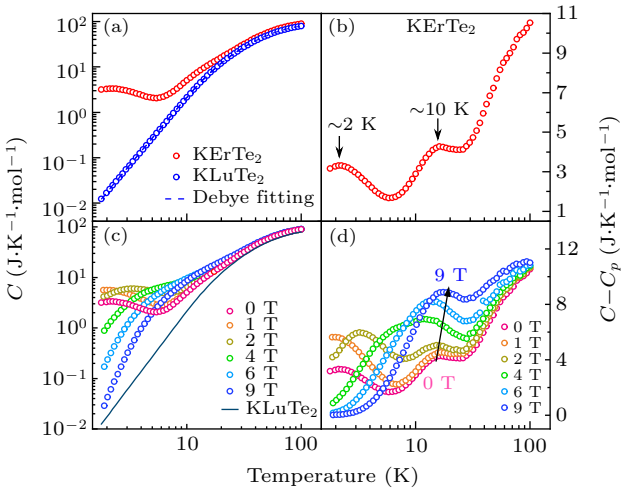


Fig. 3. (a) The zero-field heat capacities of $KErTe_2$ and $KLuTe_2$. The dashed curve is the fitting result based on the Debye model. (b) By directly subtracting the lattice contributions, other contributions to heat capacities of $KErTe_2$ are obtained. (c) The temperature-dependence of heat capacities under several different magnetic fields. (d) Same as (c) with the lattice heat capacities having been subtracted.

In order to better understand the origin of these two peaks, the field-dependent specific heat measurements were performed on $KErTe_2$ single crystals, as shown in Figs. 3(c) and 3(d). One can find that with increasing field, both these two peaks move to high temperatures and above 4 T, these two peaks overlap with each other. Such a behavior suggests that the two peaks can not be related to the spin exchange interaction since the heat capacities contributed by the spin exchange interaction will move to low temperatures with increasing magnetic field, inconsistent with our observation. Moreover, based on the Curie–Weiss fitting of the susceptibility, one can estimate that the spin exchange interaction is about 1 K, which is lower than the observed two peaks, also indicating that these two peaks do not origin from the spin exchange interaction.

Having exclude the possible origins of impurities and spin exchange interaction, we suggest that these two peaks origin from the CEF of Er^{3+}. The reason is that these two peaks exhibit the same behavior as those observed in $KErSe_2$,[35] where two broad peaks are also observed below 10 K, and move to high temperatures with increasing field. Thus, we believe that the two peaks at ~2 K and ~ 10 K have the same origin as that observed in $KErSe_2$. A quantitative understanding of these two peaks requires more theoretical work in the future and goes beyond the scope of this paper.

We further performed absorption spectrum measurements to get the charge gap of $KErTe_2$. As shown in Fig. 4, the absorption spectrum exhibits an un-saturated behavior over a wide wavelength range (from ~ 2150 nm (0.58 eV) to ~ 980 nm (1.27 eV)). Thus, the charge gap can be roughly estimated as 0.93 ± 0.35 eV. Compared with the charge gaps of other QSL candidates (see Table 3), one can find that $KErTe_2$ has the smallest charge gap. Thus, it provides a perfect platform for metallization of QSL insulators to explore the connection between QSLs and high-temperature superconductivity.

Table 3. Charge gaps of some reported QSL candidates.

Component	Charge gaps (eV)	References
$KErTe_2$	0.93	This work
$NaErSe_2$	1.86	[36]
$NaYbSe_2$	1.9	[29]
$NaErS_2$	2.29	[36]
$KErSe_2$	2.32	[36]
$NaYbS_2$	2.7	[29]
$ZnCu_3(OH)_6Cl_2$	3.3	[37]
$NaYbO_2$	4.5	[29]
$YbMgGaO_4$	>3	[16]

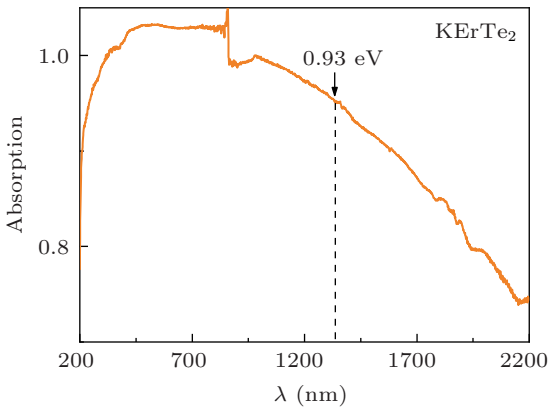


Fig. 4. The UV-Vis absorption spectrum of $KErTe_2$.

4. Summary

In conclusion, we report the successful synthesis of a new rare-earth chalcogenide compound $KErTe_2$. Specific heat and magnetic susceptibility measurements on $KErTe_2$ single crystals reveal no structural and magnetic transition down to 1.8 K, suggesting that $KErTe_2$ represents a well QSL candidate. Moreover, the absorption spectrum shows that the charge gap of $KErTe_2$ is roughly 0.93 ± 0.35 eV, which is the smallest gap among all QSL candidates. These findings suggest that $KErTe_2$ represents a QSL candidate with much small charge gap, providing a perfect platform to explore the connection between QSLs and high-temperature superconductivity by means of tuning the charge gap (for example hydrogen doping or pressure).

References

[1] Anderson P W 1973 *Mater. Res. Bull.* **8** 153
[2] Kivelson S A, Rokhsar D S and Sethna J P 1987 *Phys. Rev. B* **35** 8865
[3] Baskaran G and Anderson P W 1988 *Phys. Rev. B* **37** 580
[4] Kotliar G and Liu J L 1988 *Phys. Rev. B* **38** 5142
[5] Scalapino D J, Loh E and Hirsch J E 1987 *Phys. Rev. B* **35** 6694
[6] Monthoux P and Pines D 1993 *Phys. Rev. B* **47** 6069
[7] Lee P A, Nagaosa N and Wen X G 2006 *Rev. Mod. Phys.* **78** 17

[8] Helton J S, Matan K, Shores M P, Nytko E A, Bartlett B M, Yoshida Y, Takano Y, Suslov A, Qiu Y, Chung J H, Nocera D G and Lee Y S 2007 *Phys. Rev. Lett.* **98** 107204

[9] Han T H, Helton J S, Chu S Y, Nocera D G, Rodriguez-Rivera J A, Broholm C and Lee Y S 2012 *Nature* **492** 406

[10] Olariu A, Mendels P, Bert F, Duc F, Trombe J C, de Vries M A and Harrison A 2008 *Phys. Rev. Lett.* **100** 087202

[11] Li Y S, Liao H J, Zhang Z, Li S Y, Jin F, Ling L S, Zhang L, Zou Y M, Pi L, Yang Z R, Wang J F, Wu Z H and Zhang Q M 2015 *Sci. Rep.* **5** 16419

[12] Li Y S, Chen G, Tong W, Pi L, Liu J J, Yang Z R, Wang X Q and Zhang Q M 2015 *Phys. Rev. Lett.* **115** 167203

[13] Li Y S, Adroja D, Biswas P K, Baker P J, Zhang Q, Liu J J, Tsirlin A A, Gegenwart P and Zhang Q M 2016 *Phys. Rev. Lett.* **117** 097201

[14] Shen Y, Li Y D, Wo H L, Li Y S, Shen S D, Pan B Y, Wang Q S, Walker H C, Steffens P, Boehm M, Hao Y Q, Quintero-Castro D L, Harriger L W, Frontzek M D, Hao L J, Meng S Q, Zhang Q M, Chen G and Zhao J 2016 *Nature* **540** 559

[15] Li Y S, Adroja D, Bewlwy R I, Voneshen D, Tsirlin A A, Gegenwart P and Zhang Q M 2017 *Phys. Rev. Lett.* **118** 107202

[16] Li Y S, Adroja D, Voneshen D, Bewley R I, Zhang Q M, Tsirlin A A and Gegenwart P 2017 *Nat. Commun.* **8** 15814

[17] Banerjee A, Bridges C A, Yan J Q, Aczel A A, Li L, Stonr M B, Granroth G E, Lumsden M D, Yiu Y, Knolle J, Bhattacharjee S, Kovrizhin D L, Moessner R, Tennant D A, Mandrus D G and Nagler S E 2016 *Nat. Mater.* **15** 733

[18] Banerjee A, Yan J Q, Knolle J, Bridges C A, Stone M B, Lumsden M D, Mandrus D G, Tennant D A, Moessner R and Nagler S E 2017 *Science* **356** 1055

[19] Cao H B, Banerjee A, Yan J Q, Bridges C A, Lumsden M D, Mandrus D G, Tennant D A, Chakoumakos B C and Nagler S E 2016 *Phys. Rev. B* **93** 134423

[20] Ran K J, Wang J H, Wang W, Dong Z Y, Ren X, Bao S, Li S C, Ma Z, Gan Y, Zhang Y T, Park J T, Deng G C, Danilkin S, Yu S L, Li J X and Wen J S 2017 *Phys. Rev. Lett.* **118** 107203

[21] Leahy I A, Pocs C A, Siegfried P E, Graf D, Do S H, Choi K Y, Normand B and Lee M 2017 *Phys. Rev. Lett.* **118** 187203

[22] Shirata Y, Tanaka H, Matsuo A and Kindo K 2012 *Phys. Rev. Lett.* **108** 057205

[23] Zorko A, Nellutla S, van Tol J, Brunel L C, Bert F, Duc F, Trombe J C, de Vries M A, Harrison A and Mendels P 2008 *Phys. Rev. Lett.* **101** 026405

[24] Li Y D, Shen Y, Li Y S, Zhao J and Chen G 2018 *Phys. Rev. B* **97** 125105

[25] Li Y D and Chen G 2017 *Phys. Rev. B* **96** 075105

[26] Zhu Z Y, Maksimov P A, White S R and Chernyshev A L 2017 *Phys. Rev. Lett.* **119** 157201

[27] Zhu Z Y, Maksimov P A, White S R and Chernyshev A L 2018 *Phys. Rev. Lett.* **120** 207203

[28] Kimchi I, Nahum A and Senthil T 2018 *Phys. Rev. X* **8** 031028

[29] Liu W W, Zhang Z, Ji J T, Liu Y X, Li J S, Wang X Q, Lie H C, Chen G and Zhang Q M 2018 *Chin. Phys. Lett.* **35** 117501

[30] Baenitz M, Schlender P, Sichelschmidt J, Onykiienko Y A, Zangeneh Z, Ranjith K M, Sarkar R, Hozoi L, Walker H C, Orain J C, Yasuoka H, van den Brink J, Klauss H H, Inosov D S and Doert T 2018 *Phys. Rev. B* **98** 220409

[31] Ding L, Manuel P, Bachus S, Gru?ler F, Gegenwart P, Singleton J, Johnson R D, Walker H C, Adroja D T, Hillier A D and Tsirlin A A 2019 *Phys. Rev. B* **100** 144432

[32] Ranjith K M, Dmytriieva D, Khim S, Sichelschmidt J, Luther S, Ehlers D, Yasuoka H, Wosnitza J, Tsirlin A A, Kühne H and Baenitz M 2019 *Phys. Rev. B* **99** 180401

[33] Bordelon M M, Kenney E, Liu C X, Hogan T, Posthuma L, Kavand M, Lyu Y, Sherwin M, Butch N P, Brown C, Graf M J, Balents L and Wilson S D 2019 *Nat. Phys.* **15** 1058

[34] Zhang Z, Ma X L, Li J S, Wang G H, Adroja D T, Perring T P, Liu W W, Jin F, Ji J T, Wang Y M, Kamiya Y, Wang X Q, Ma J and Zhang Q M 2021 *Phys. Rev. B* **103** 035144

[35] Xing J, Sanjeewa L D, Kim J, Meier W R, May A F, Zheng Q, Custelcean R, Stewart G R and Safat A S 2019 *Phys. Rev. Mater.* **3** 114413

[36] The data come from https://atomly.net

[37] Pustogow A, Li Y, Voloshenko I, Puphal P, Krellner C, Mazin I I, Dressel M and Valentí R 2017 *Phys. Rev. B* **96** 241114